INTERMEDIATE ANNOTATIONLESS DYNAMICAL OBJECT-INDEX BASED QUERY IN LARGE IMAGE ARCHIVES WITH HOLOGRAPHIC REPRESENTATION[1]

Javed I. Khan

Contact:

Department of Electrical Engineering
493 Holmes Hall, 2540 Dole Street
University of Hawaii at Manoa
HI-96822, USA

Phone: (808)-956-3868
Fax: (808)-941-1399
javed@hawaii.edu

SUMMARY

This paper presents a new parallel and distributed associative network based technique for content-based image retrieval (CBIR) with dynamic indices. Unlike any prior artificial associative networks (AAM), this new associative search network has the unique ability to explicitly focus on any subset of pixels in the image. It can also provide a feedback meta-quantity on the quality of outgoing information. The network is founded on a bi-modal representation of information elements which in addition to basic information also includes meta-states. Its computational model has been derived from optical holography. These unique capabilities coupled with usual advantages of associative computing (adaptability, efficiency, ability to cope with imprecision, parallel and distributed mode of computation) now for the first time makes it possible to realize a CBIR technique based on associative computing. This new CBIR strategy provides an inquirer greater flexibility to independently and dynamically construct object-indices without depending on the fixed, pre-defined adhoc indices used by traditional CBIR approaches. The paper presents the mechanism, architecture and performance of an image archival and retrieval system realized with this new network.

1 This manuscript has been accepted for publication in the **Journal of Visual Communication and Image Representation** for its special Issue on Indexing, Storage, Retrieval and Browsing of Image and Video and will appear in Vol 7, no 4, in 1997.

INTERMEDIATE ANNOTATIONLESS DYNAMICAL OBJECT-INDEX BASED QUERY IN LARGE IMAGE ARCHIVES WITH HOLOGRAPHIC REPRESENTATION

Javed I. Khan

Laboratories of Intelligent and Parallel Systems
Department of Electrical Engineering
University of Hawaii at Manoa, USA
javed@hawaii.edu

ABSTRACT

This paper presents a new parallel and distributed associative network based technique for content-based image retrieval (CBIR) with dynamic indices. Unlike any prior artificial associative networks (AAM), this new associative search network has the unique ability to explicitly focus on any subset of pixels in the image. It can also provide a feedback meta-quantity on the quality of outgoing information. The network is founded on a bi-modal representation of information elements which in addition to basic information also includes meta-states. Its computational model has been derived from optical holography. These unique capabilities coupled with usual advantages of associative computing (adaptability, efficiency, ability to cope with imprecision, parallel and distributed mode of computation) now for the first time makes it possible to realize a CBIR technique based on associative computing. This new CBIR strategy provides an inquirer greater flexibility to independently and dynamically construct object-indices without depending on the fixed, pre-defined adhoc indices used by traditional CBIR approaches. The paper presents the mechanism, architecture and performance of an image archival and retrieval system realized with this new network.

Key Words: Associative Memory, Content-based Retrieval, Attention.

1 INTRODUCTION

Content-Based Retrieval: The enormous growth of the image repositories over the last decade, spurred by the rapid advancement in image capture and sensor technology, has made content based search one of the most critical challenges in the area of intelligent image information management [27,28]. *Astronomy, satellite imagery, geographical information systems* [3,5,23], *medical diagnostics* [25], *educational archives* [7], *criminology, patent management* [26], *journalistic image repository* [24] are just a few of the overwhelmed clientele with growing stockpiles of image databases in desperate need of effective means for content-based search.

Content-based image retrieval (CBIR) refers to a technique where images are identified from a piece of it. Generally, these index pieces refers to an object (or combination) denoted by a set of pixels. It is expected that a match should be based on the similarity between these objects.

For instance, a radiologist can request for kidneys that are not of the normal shape like the one in a given example image. A detective often needs to find if there is any recorded image which matches some interesting ridge patterns of a fingerprint at hand. However, the problem is that these image objects and concepts are perceptual and subjective.

Nature of Image Information: Image information is representationally sparse and distributed and the process of it's perceptualization involves complex abstraction. The more an image is non graphical[2] (such as medical images),

2 Although, both graphical and natural images are sensed visually, possibly the process involved in the perceptualization is significantly different [13]. In a relative sense, graphical images (such as textual writings, engineering drawing) are more pre-abstracted, and convey refined information.

the concepts in it, objects (such as a tumor) and their relationships (such as anatomical, compositional, or spatial relations), tend to be increasingly subjective both in the senses of concreteness of their definability and precision of their measurability.

Other Retrieval Techniques: Because of the high cost of searching into actual images, in recent years a number of techniques have been developed which can perform pseudo-content-based retrieval. These approaches rely on annotated symbolic model of the 'content' of images to mediate the search. Chabot [27], MACS [27], QBIC [16], Piction [27], IIDS [3], PICQUERY [11], IDB [21] are few examples of such experimental systems that have been developed over the years. The specific ways in which these approaches build and manage the intermediate model of content vary. These techniques mostly use textual representations (natural language or keywords) in terms of a set of pre-decided attributes (color, shape, size, etc.) and their values [22,7,6]. Some others use machine detectable features (geometric moments, triangular cover, points of maximum curvature, etc.) to help in automating the extraction process [9, 17, 16]. These symbolic descriptions are then stored into some form of data structures (ranging from plain text [7], complex semantic net [22], relational database [29] to ingenious 2D-string [3]). Once such descriptive models are available, variants of conventional algorithmic database search techniques are used to search them.

However these psudo-content-based retrieval techniques face some limitations because of their fundamental dependance on such intermediate models of "meaning" [13, 2, 5]. In the first level, it is difficult to design a sufficient annotation language that can contain all the possible ranges of meaning. In the second level, even assuming the designability of such a language, the process of model extraction or interpretation itself seems to be an indefinite and imprecise task.

While some visual concepts may be determinable during encoding, most are not indexable by any static strategy. Consequently, these pseudo-content-based retrieval techniques can be used only for applications where images are near graphical and the archive is slow growing, static and small, allowing the luxury of extensive domain-specific modeling and tedious human involvement. Some innovative technique is much needed to deal with a majority of applications where none of the above applies.

In this paper we present an alternate approach for content based retrieval which can support dynamic object-indices formed by the inquirer and can overcome the above limitations of the psudo-content based retrieval methods. It is based on direct visual similarity and does not require any adhoc intermediate modeling of "meaning", rather allows the individual inquirer (also referred as the user) to attach their own "meaning" dynamically during query. However, if necessary, it can accept encoding time interpretations. The search engine of this approach is based on a new associative computing model.

Associative Computing: Parallel and distributed models of Artificial Associative Memory (AAM) evolved from the phenomenal advancement of neural network research demonstrate two interesting characteristics which strongly suggest their potential applicability for content-based retrieval [8,13] based on direct similarity. These models are adaptive and thus can avoid the need for explicit symbolic model extraction. Also, computationally they are fast[3], inherently distributed and parallel, and thus can offer direct search ability into images. Because of such appealing

3 Various classical pattern matching algorithms exists to find exact match in a pattern string. However these classical methods are impractical for large volume images. Because the multidimensional and indefinite nature of feature space makes it almost impossible to pre-order (sort) images that improves the search efficiency of these methods [20].

characteristics, it has long been anticipated (almost from the days of the advent of neuro computing) that AAMs can be potentially used for content-based retrieval of image information [8]. However, no such system has actually been implemented with success yet.

One of the reasons for such lack of success is that current AAMs do not have the ability to focus on visual objects or more specifically on any "meaningful" subset of the pixels in the images denoting the visual object(s). During encoding, these models nonchalantly assume all the pixels in the image as equi-important. During query, they emulate a similar indiscriminate **statistical pixel-to-pixel** distance evaluation (mean square error, entropy etc.) giving equal importance to all the pixels in the sample image. Neither the encoder nor the searcher has any control over the importance of the pixels to draw attention to any particular subset of pixels, which makes current AAMs rather simplistic to be used for image retrieval.

Role of Selective Search in CBIR: This paper explores how a new associative computing paradigm can remedy these long-standing limitations of AAMs, and can be applied for visual object oriented encoding and content-based retrieval in image archives [6,10]. The technique presented in this paper is based on a new computing paradigm called *Multidimensional Holographic Associative Computing (MHAC)* which can perform a form of object oriented image encoding and query based on similarity of objects in a sample image. Before presenting this model, the role of focus in pattern space at various stages of CBIR is explained to illustrate what fundamental improvements are needed in current AAMs.

(1) *Attention in Encoding:* The meta-control over the importance of pixels is critical for any search based on object similarity both during encoding and recalling. As an example, in a CT-scan image, a not so cognitive-wise significant region (such as empty outside) can be statistically quite dominant for its large cover, while an organ with important cognitive significance may be statistically insignificant for its small size. Logically, such a problem can be alleviated by encoder's prior-knowledge of the cognitive importance of the segments. But any matching strategy, which can not accommodate such meta importance but relies solely on the statistical importance of a feature or object (such as conventional AAMs) can not handle these situations.

(2) *Attention in Decoding:* The ability to focus during query is also critical. A sample image can be interpreted in numerous ways based on the visual object(s) in it that the searcher wants to emphasize as a basis for similarity. Each interpretation may result in different answers. For example, in a sample CT image depicting an abdominal cross-section the searcher may choose either the "spinal column" or a "tumor" as his/her basis of similarity. But, current AAM models cannot accommodate such dynamic (post-learning) specification of focus. It always converges only to the statistically closest match based on all the pixels of the sample. One of the consequences of such inability to focus, is that the cues must be statistically significant, which is also unrealistic. In Conventional AAMs the cue is required to be at least 50% of the query frame for correct retrieval [12,19]. The critical index objects used in image search as a cue are always based on their cognitive importance irrespective of their statistical dominance. Such a cue is quite often only a fraction of the entire image.

(3) *Feedback Attention in Retrieval:* Since an image matching memory receives imperfect information, it is natural to assume that the information coming out of the memory would also be imperfect. It is therefore important that the memory should also have a mechanism to generate a reciprocal feedback on the quality of outgoing information. The critical role of such feedback can be explained through a trivial scenario in pattern matching. Let us consider a memory that has learned a few image patterns. Now during query, if a sample pattern is presented, and if it resembles none of the learned ones, still a pattern will emerge at the output(s) of the memory. Now the problem is that (unless it can be compared with all the stored images) there is no way of identifying if this retrieved pattern has ever been learned.

Any effective pattern search process always requires a mechanism to convey response equivalent to "no match" or more formally some assessment on the quality of match. It is a meta information and is distinct from the pattern information. Current AAMs are unable to provide such assessment.

In this paper a new associative computational mechanism[4] will be shown which demonstrates this critical ability of attention localization in all three of the above forms and which also retains the usual advantages of associative computing (adaptability, efficiency, ability to cope with imprecision, parallel and distributed mode of computation).

This computational model is physically a conceptual generalization of optical holographic principles [4] and computationally an instance of associative memory. This paper explains its operations both analytically and empirically. Section 2 first defines the conceptual and computational model. Section 3 then explains how this model processes the above three forms of meta-information. Finally, Section 4 and 5 experimentally demonstrate a content-based image pattern matching system based on this memory.

2 HOLOGRAPHIC MEMORY

Multidimensional Holographic Associative Computing (MHAC), inspired by optical holography, has this critical ability to focus in all three of the above identified forms.

At the conceptual level, even more compelling and distinguishing aspect of this memory is its representation. It embodies a premise that any information processing system (such as a memory) which intend to effectively deal with imperfect information, in addition to the basic information, should incorporate meta-information pertaining to the status of base information within its computational framework. Although simple, this premise is profoundly different from traditional symbolic or neural approaches. The traditional symbolic systems do not require this added burden because of the perfection of the dealt information. Current neural (and associative) systems attempt to handle nonconformity by discovery of statistical significance in the dealt information. However in many applications (including content-based image retrieval) the effective significance may not be expressed in pure statistics[5].

This memory model is based on a new formalism which assumes the *trust* in each piece of transacted information as inherently non-conformal. In addition to the basic *measurements*, the formalism includes the *meta-information* about the status of each given piece of measurements as an integral part of its representation and computation. Below, the conceptual model of this bi-modal memory is presented.

2.1 Bimodal Associative Memory

Let a stimulus pattern be denoted by a symbolic vector $S^{\mu} = \{s_1^{\mu}, s_2^{\mu}, \ldots . s_n^{\mu}\}$. Each of the individual elements in this vector represents a piece of *information* (subscript refers to the element index and superscript refers to pattern index). The values of these elements correspond to a measurement obtained by some physical sensor.

4 Although, current AAMs demonstrate attractive computational characteristics suitable for handling image information compared to traditional algorithmic approaches, but none of these meta-information processing capabilities can be easily realized on them.

5 In this sense, conventional neural associative computing hides imperfection in input information, rather than dealing with it. It attempts to completely fix the imperfection in the input with brute statistical analysis and to generate "perfect" output (it has no representation to express doubt in its output), rather than accepting the fact that imperfection "in" means imperfection "out".

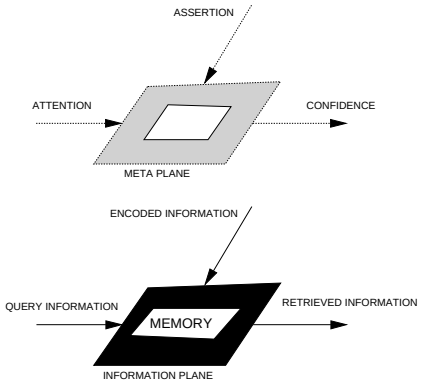

Fig-1 Flow of Information In and Out of a Memory and Meta-Information

Any memory has three information channels (as shown in the bottom plane of Fig-1). The first is the encoder, where information is received during learning. The second is the decoder, where query template information is received from the inquirer. The third is the output channel, where for each query, the memory generates the response.

A conventional memory processes only the above measurement components of the involved information elements. In contrast, the novel formalism we would like to propose adopts an additional meta-knowledge plane (as shown in the upper plane in Fig-1) to accommodate dynamic attention.

Thus, in this new formalism each information element is modeled as a bi-modal pair $s_k^{\mu} = \{\alpha_k^{\mu}, \beta_k^{\mu}\}$. Where α represents the *measurement* of the information elements and β represents the *meta-knowledge* associated with it. The linguistic interpretation to the quantities of this meta-plane varies depending on the channel. For the encoding channel this meta-knowledge corresponds to a form of *assertion* from the encoder. For the query pattern it corresponds to a form of *attention* on the part of the inquirer. For the memory response it corresponds to the *confidence* on the retrieved information as assessed by the memory itself. These terms will be used hereafter in this paper.

Having identified this conceptual model, now we will show how this bi-modal memory can be efficiently realized based on a computation model derived from optical holography with all the usual advantages of associative computing.

2.2 Optical Holography

Let us consider a simplified version of the hologram synthesis process. As shown in Fig-2, imagine two wavefronts incident on a medium in plane P. Let one of these be a plane wave of light (at an angle to the optical axis) indicated by $S = K.e^{-j\alpha x}$, and the other be the wavefront $R(x, y)$, that contains the complex variations to be encoded on the hologram. If the two wavefronts are coherent (such condition is generally met by using a single LASER source, mirrors and beam splitters), then the intensity incident on plane P is given by (bar indicates complex conjugation):

$$\begin{aligned} I(x,y) &= |\, R(x,y) + Ke^{-j\alpha x} \,|^2 \\ &= |\, R(x,y) \,|^2 + K^2 + K\overline{R}(x,y)e^{-j\alpha x} + KR(x,y)e^{+j\alpha x} \\ &= I_A + I_B + I_C + I_D \end{aligned} \quad \ldots.(1)$$

Consequently, the medium used in plane P will have a transmittance t(x,y) that is proportional to I(x,y).

Interestingly, the encoded wavefront R(x,y) can now be retrieved from the hologram t(x,y), if we reilluminate it by the stimulus wavefront that was used in the hologram recording process. For such illumination, the light leaving the hologram in Fig-2 is given by:

$$O(x,y) = t(x,y).Ke^{-j\alpha x} = K.I(x,y)e^{-j\alpha x}$$
$$= K(K^2 + |R(x,y)|^2)e^{-j\alpha x}$$
$$+K^2\overline{R}(x,y)e^{-j2\alpha x} + K^2R(x,y)$$
$$= (A+B)+C+D \quad \ldots.(2)$$

Due to the diffraction on the holographic plate three beams leave the holographic plate in three directions. A viewer placed in the direction of D sees only the wavefront R(x,y). This is exactly the one that was supposed to emerge from the real object. This wavefront creates two slightly different images in the two eyes of the viewer, just in the way the actual R(x,y) directly reflected from the object would have created. As a result when the viewer looks towards the holographic film he/she sees the hologram of the actual object in its original place with all its 3-D feel. The same hologram can be used to obtain the wavefront S from R(x,y) in almost the same manner. These ideas were originally suggested by Gabor in Late 40's [4]. The actual 3D hologram had to wait 10 years till the perfection of LASER.

Associations between Objects: Hologram can also store association between a pair of objects. If instead of the plain wave, now the light reflected from a second object placed in the scene becomes the stimulus wave $S(x,y)$, then the interference pattern created on P stores the association between these pair of objects. If the plane P is reilluminated by the light reflected from one of the objects then the light leaving the plane becomes the one reflected from the other. Hologram has two additional characteristics which make it even more interesting.

Multiple Associations: The first among these is the ability to store multiple associations on the same holographic film. An interference pattern incident from a second pair of objects can now be super imposed on the earlier interference pattern on plane P. If any of these four objects is used to reilluminate the holograph, then the recollected wavefront looks like the one associated with this object. A large number of associations between object pairs thus can be stored on the same photographic film.

Robustness: The other interesting property of hologram is its ability to reconstruct the image from partial information. During recording, each point on plane P receives a reflected beam from all the points of both the objects. At the same time the illuminating beam reflected from each point of both the objects reaches all the points on P. During retrieval, each point of P illuminated by each reflected beam from S(x,y) independently reconstructs the original wavefront R(x,y).

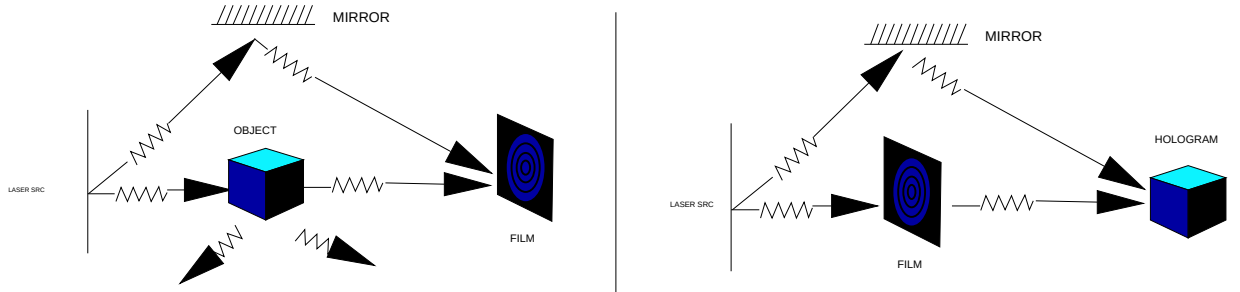

(a) Encoding **(b) Decoding**

Fig-2 Recording and Decoding in Holography

The effect of such independence is twofold. First, if only a part of the hologram film is used, even then the actual R(x,y) is reconstructed (except for a slight loss of the viewing angle). The hologram also has robustness in a different sense. Instead of dividing the film, if only a part of the stimulus beam S(x,y) is used to illuminate the film (and the rest is blocked), even then the original wavefront R(x,y) appears (except for some loss in brightness).

The Phenomena of Holography: The properties associated with the hologram are extremely intriguing to our senses. Here we will try to list them. In essence a hologram can (i) record and accurately regenerate 3D complex waveforms, (ii) learn associations between two waveforms, (iii) enfold enormous number of multiple associations, (iv) regenerate waveforms from a part of the hologram film, and finally (v) regenerate waveforms even when excited by a partial stimulus wavefront. The implications of these fascinating characteristics for us can be stated in the following way.

It is the first property which makes hologram a 3D waveform recording medium (for which it is most famous). The addition of second property makes it a memory. Further addition of the third property makes it an associative memory. Similarly, the fourth property makes it a distributed associative memory. Finally, the last property makes it a distributed associative memory with the ability to focus. Next, the essential computations of holography which can yield all five of these properties digitally are identified.

Essence of the Computation: As evident by now, the key to the reconstruction process lies in the 3rd and 4th terms of (1). A real hologram operates with two constraints; the first one is (i) that the optical setup performs addition of two wavefronts and the other one is (ii) that the recording medium can store only positive valued functions. But a computer can easily evaluate products and store complex-valued spatial functions. Therefore, the 3rd term is directly captured and the 4th term is evaluated if needed since it is conjugate of the 3rd. The above simplification not only reduces the amount of data that has to be stored in the medium but also eliminates the interference from some of the unwanted terms. I_D retains all the critical properties of a holography.

2.3 Computational Representation

As evident, one of the key features of optical holography is how information is being represented. In optical holography an element of the pattern is represented as optical waveforms which is a 2D complex value. Such a representation can be directly used for building a bi-modal memory. However, since we are not restricted by optics, we adopt a slightly generalized formalism. Instead of using 2D numbers, we represent the elements in the form of *multidimensional complex numbers* (MCN) as a point on the surface of a hypersphere. In this formalism, the MCN phase represents the *measurement* and magnitude represents the *meta-knowledge* component of each piece of information. Thus:

$$s_k = (\alpha_k, \beta_k) \Rightarrow \lambda_k e^{\left(\sum_j^{d-1} \hat{i}_j \theta_{j,k}\right)}$$

Here, each α_i^k is mapped onto an angular span defined by the phase elements θ_i^k in the range of $\pi \geq \theta \geq \pi$ through a suitable transformation, where each $s(\lambda_k, \theta_1^k, \theta_2^k, \ldots \theta_{d-1}^k)$ is a d-dimensional vector. Each of the θ_j^k is the spherical projection (or phase component) of the vector along the dimension $\hat{i}_j$. λ_k becomes the magnitude of this vector. Thus, a stimulus with *n* elements and a response with *m* elements are represented respectively as:

$$[S^\mu] = \left[\lambda_1^\mu e^{\left(\sum_j^{d-1} \hat{i}_j \theta_{j,1}^\mu\right)}, \lambda_2^\mu e^{\left(\sum_j^{d-1} \hat{i}_j \theta_{j,2}^\mu\right)}, \ldots . \lambda_n^\mu e^{\left(\sum_j^{d-1} \hat{i}_j \theta_{j,n}^\mu\right)} \right]$$

$$[R^\mu] = \left[\gamma_1^\mu e^{\left(\sum_j^{d-1} \hat{i}_j \phi_{j,1}^\mu\right)}, \gamma_2^\mu e^{\left(\sum_j^{d-1} \hat{i}_j \phi_{j,2}^\mu\right)}, \ldots . \gamma_m^\mu e^{\left(\sum_j^{d-1} \hat{i}_j \phi_{j,m}^\mu\right)} \right]$$

Here, in the response pattern the phasor ϕ represents the measurement of the expected associated response pattern elements from the memory system, and γ represents the expected system confidence on ϕ.

2.4 Encoding

The operations are similarly generalizations of (1) and (2). Like the 3rd term of (1), an association is constructed by the outer product of the two complex waveforms. Associations are superimposed. The association between each individual stimulus and its corresponding response is computed as follows.

$$[X^{\mu}] = [\overline{S}^{\mu}]^{T} \cdot [R^{\mu}]$$

The associations derived from a set of stimuli and a set of corresponding responses are superimposed on a super matrix X which is referred as Holograph. If the size of the stimulus and response patterns are *n* and *m*, then the size of the holograph matrix is *mxn*.

$$[X] = \sum_{\mu}^{P} [X^{\mu}] = \sum_{\mu}^{P} [\overline{S}^{\mu}]^{T} [R^{\mu}] \qquad \ldots.(3)$$

2.5 Retrieval

During recall, an excitory stimulus pattern $[S^e]$ is obtained from the query pattern:

$$[S^e] = \left[\lambda_1^e e^{\left(\sum_j^{d-1} i_j \theta_{j,1}^e \right)}, \lambda_2^e e^{\left(\sum_j^{d-1} i_j \theta_{j,2}^e \right)}, \ldots . \lambda_n^e e^{\left(\sum_j^{d-1} i_j \theta_{j,n}^e \right)} \right]$$

The decoding operation is similarly performed as follows:

$$[R^e] = \frac{1}{c} [S^e] \cdot [X] \qquad where, \quad c = \sum_{k}^{n} \lambda_k \qquad \ldots.(4)$$

In section 3, we show how this model also can support all three forms of meta-information. As expected, this new computational model has advantages similar to the conventional AAMs. In fact, as shown in equation (4), a search into thousands of stored images through this technique requires a single complex matrix multiplication.

Use of complex number is not a new concept in artificial associative computing, at least in 2-dimensions. In 1990, Sutherland [18], in his pioneering work presented the first truly holographic associative memory with learning algorithm analogous to the correlation learning used here. It is a 2-dimensional special case of the generalized multi-dimensional phasor representation introduced here. Recently, Timothy Masters [9] also reported another 2D-complex valued network with a learning algorithm analogous to Backpropagation. However both of these attempts remained focused on their network's efficiency issues as a conventional adaptive filter, without exploring the fundamentally different attention phenomenon associated with such representation. Now the capability of processing assertion, attention, and confidence is explained next.

3 ATTENTION, ASSERTION and CONFIDENCE

3.1 Basics

By combining the encoding and decoding operations expressed in equations (3) and (4), the retrieved association is given by equation (5). Here, the retrieved response is decomposed into two components, one is the *principal component*, which is the response generated from the association which is closest to the query stimulus $[S^e]$. The other is the *crosstalk component*, which accounts for the effect generated from rest of the associations.

$$[R^e] = \frac{1}{c} \cdot [S^e] [\overline{S}^t]^T [R^t] + \frac{1}{c} \cdot \sum_{\mu \neq t}^{P} [S^e] [\overline{S}^{\mu}]^T [R^{\mu}] = [R^e_{principal}] + [R^e_{crosstalk}] \qquad \ldots.(5)$$

Here $[S^t]$ represents the candidate match. The specific characteristics for the crosstalk and the principal components are derived next.

3.2 Principal Component

Lemma 1: *If the excitatory stimulus* $[S^e]$ *bears similarity to any previously encoded stimulus* $[S^t]$*, in their* α*-suit then the principal component of generated response* $[R^e]$ *resembles its corresponding response pattern* $[R^t]$*.*

Proof: First, the principal component given by equation (5) will be analyzed to estimate the λ of the recalled response in terms of the closeness of the query stimulus S^e and the candidate match with a previously encoded pattern S^t. Let us consider the retrieval of the j^{th} component of the response. Other response components are retrieved independently in identical manner. It is also assumed that all the encoded stimulus patterns have $\lambda = 1$ without any loss of generality.

$$r^e_{j(principal)} = \frac{1}{c}[S^e][\overline{S}^t]^T r^t_j$$

$$= \frac{1}{c}\sum_k^n \lambda^t_k \cdot \lambda^e_k \cdot e^{\left(\sum_j^{d-1} \hat{i}_j\left(\theta^e_{j,k} - \theta^t_{j,k}\right)\right)} \cdot r^t_j \qquad \ldots(6.1)$$

If the query stimulus, and the target stimulus corresponds closely, then $\theta^t_{j,k} \to \theta^e_{j,k}$. Thus, all the exponent terms become unity with no phase disturbance. Which, reduces to,

$$r^e_{j(principal)} \cong \frac{1}{c}\sum_k^n \lambda^e_k \cdot \lambda^t_k \cdot r^t_j \qquad \ldots.(6.2)$$

The phase of the retrieved response corresponds to the retrieved information, and is equivalent to the phase of the encoded response:

$$argc(r^e_{j(principal)}) \cong argc(r^t_j) \qquad \ldots.(6.3)$$

.

3.3 Crosstalk Component

Lemma 2: *For sufficiently symmetrical distribution of the stimulus and response patterns, the magnitude of the crosstalk component tends to be zero.*

Proof: The crosstalk component can be thought of as a summation of a set of randomly oriented d-dimensional vectors. Let us, consider uni-normal projection of a set of such vectors $\vec{A}_\mu$,

$$r^e_{crosstalk} = \frac{1}{c}\cdot\sum_{\mu \neq t}^P [S^e][\overline{S}^\mu]^T [R^\mu] = \frac{1}{c}\cdot\left\{\sum_{\mu \neq t}^P \vec{A}_\mu\right\}$$

Let the d-dimensional vector is represented as:

$$\vec{A}_\mu \equiv A(\theta^\mu_1, \theta^\mu_2, \ldots \theta^\mu_{d-1}) \equiv A(x^\mu_1, x^\mu_2, \ldots x^\mu_d)$$

If the phases are symmetrically distributed, i.e., the distribution functions $f_\theta(x) = f_\theta(\pi - x)$ in the $0 - 2\pi$ range, then,

$$E\{\cos\theta\} = \int \cos x f_\theta(x) dx \to 0 \qquad E\{\sin\theta\} = \int \sin x f_\theta(x) dx \to 0$$

Which implies that,

$$r^{e}_{crosstalk} = \frac{1}{c}.\left\{ \sum_{\mu \neq t}^{P} \vec{A}_{\mu}^{d} \right\} \cong 0 \qquad \ldots.(proved)$$

For effective operation of MHAC, the magnitude of the cross-talk component should be kept sufficiently small compared to the principal component in practice. The actual value of this term depends on (i) the distribution function $f_{\theta}()$ and (ii) average magnitude of $\vec{A}_{\mu}^{d}$s. An interesting point to note here is that the performance of holographic memory depends more directly on the symmetry in the distribution function. Symmetrical distribution of the vectors and lower assertion values have the effect of keeping the saturation low[6], lowering recall noise and improving capacity.

The above two lemmas together explain how the above computation mechanism can act as an associative memory.

3.4 Attention and Assertion Characteristics

In this section now it is shown that how this computational framework processes the two inflow meta-quantities; *attention* and *assertion*. Lemmas 3 and 4 explain the attention and assertion control mechanism of it.

Lemma 3 (Assertion Control): *Given an encoded stimulus* $[S^t]$ *with unequal analog distribution of assertion of its element field specified by* $\Lambda^t = [\lambda_1^t, \lambda_2^t, \ldots, \lambda_n^t]$*, and the memory dynamics specified by equations (3) and (4), the elements of the target pattern will contribute in the reconstruction of the target pattern* $r^{e}_{j(principal)}$ *in monotonic proportion based on the weighted importance specified in* Λ^t.

Lemma 4 (Attention Control): *Given a query stimulus* $[S^e]$*, with unequal analog distribution of attention distribution of its element field specified by* $\Lambda^e = [\lambda_1, \lambda_2, \ldots, \lambda_n]$*, the memory dynamics specified by equations (3) and (4) retrieves the pattern which best resembles* $[S^e]$*, where, individual query elements contributes in the matching in monotonic proportion based on the weighted importance specified in* Λ^e.

Proofs: As evident in (6.1), the phase of the reconstructed response $r^{e}_{j(principal)}$ is in effect a weighted average of the individual encoded responses r_j^t associative with individual element locations where the contribution of each term is weighted by both λ_k^t and λ_k^e. By adjusting individual λ_k^t's the contribution of each encoded stimulus element can be controlled during learning. A high λ_k^t will allow the k^{th} term to contribute more in the phase average, and vice versa. At the extreme, setting λ_k=0 will completely attenuate this term. But, such analog control will have no multiplicative distortion effect on the phase plane. This mechanism corresponds to the process of learning with changeable assertion. In a similar way, by adjusting individual λ_k^e's the contribution of each query stimulus element can be controlled during query. This mechanism corresponds to the process of retrieval with changeable attention. ... *(proved)*.

As can be noted, within the region of focus (either by assertion or attention) the match is still "statistical" like conventional AAMs. Thus, it maintains the usual error tolerance of AAMs.

3.5 Confidence Characteristics

Finally, now it is shown that how the above computational framework can reconstruct a measure of match as a fundamental part of bi-modal representation. This measure of match is named *mean normalized confidence* (MNC).

---

6 The symmetry of various correlated element distribution can be improved by various mapping [12].

Lemma 5 (Confidence Feedback): *Given a query stimulus* $[S^e]$*, the memory dynamics specified by equation (4.3) and (4.5) satisfies the expected relation between the quality of match and the output distribution of confidence of generated response pattern* $[R^e]$ *specified as vector* $\hat{\Lambda}^e = [\hat{\lambda}_1, \hat{\lambda}_2, \ldots, \hat{\lambda}_n]$*of corresponding element magnitudes stated in table-1.*

Proof: Let us consider the magnitude of the response elements $\hat{\lambda}_j^e$. The same results can be extended for other $\hat{\lambda}_j^e$. Let us consider that $P(a \times b, i)$ is the hyperplane spanned by the i^{th} elements of the a^{th} and b^{th} patterns. The orientation angle of element s_i^a in this plane will be denoted by $\psi_i^a \mid_{P(a \times b, i)}$. The difference between the orientation angles signifies the direct angular span between the elements s_i^a and s_i^b. Let us also define,

$$\phi_{k-l}^{e-\mu} = [\psi_k^e \mid_{P(e \times \mu, k)} - \psi_k^\mu \mid_{P(e \times \mu, k)}] - [\psi_l^e \mid_{P(e \times \mu, l)} - \psi_l^\mu \mid_{P(e \times \mu, l)}]$$

It denotes the difference between the angular spans between the k^{th} and l^{th} elements of the query (denoted as e^{th}) and μ^{th} stimulus patterns, then it can be shown through some straightforward trigonometric manipulation that:

$$\hat{\lambda}_j^e = \frac{1}{c}\sqrt{\sum_k^n (\lambda_k)^2 + \sum_k^n \sum_{l \neq k}^n \lambda_k \lambda_l \cos\phi_{k-l}^{e-t}} \text{ assuming } \mid r_j^t \mid = 1$$

$$\text{since, } c = \frac{1}{\sum_k^n \lambda_k},$$

$$= \frac{1}{c}\sqrt{\left(\sum_k^n \lambda_k\right)^2 + \sum_k^n \sum_{l \neq k}^n \lambda_k \lambda_l (\cos\phi_{k-l}^{e-t} - 1)} = \sqrt{1 + \frac{\sum_k^n \sum_{l \neq k}^n \lambda_k \lambda_l (\cos\phi_{k-l}^{e-t} - 1)}{\left(\sum_k^n \lambda_k\right)^2}} \quad \ldots.(7)$$

Let us define a distance measure between two patterns d such that, α-suit elements of the query stimulus $[S^e]$ and encoded stimulus $[S^t]$ are bounded by the distance d over the entire set, such that $\mid \psi_j^e - \psi_j^t \mid \leq d$, for all j, which implies $0 \leq \mid \phi_{k-l}^{e-t} \mid \leq 2d$.

If $d \to 0$, then the right term of (7) becomes zero, which indicates that irrespective of distribution of δ in the query pattern, $\lambda_j^r \to 1$. On the other hand, if $d \gg 0$, indicating greater distance between the patterns, then right term of (7) becomes increasingly negative ($(\cos\phi - 1) \ll 0$), which indicates the decay of λ_j^r. *...(proved).*

The decay characteristic is cosine natured. For small perturbation, λ_j^r decays very little from unity indicating statistical robustness. However the decay becomes sharper as the distance between the patterns increases. As shown by (4.11), for large d, the rate of decay is modulated by the asymmetry in the distribution of λ-suit in the query.

4 IMAGE ARCHIVAL and RETRIEVAL SCHEME

Now a scheme is described for object-oriented image encoding and retrieval using MHAC. Fig-3 outlines the scheme. In its simplest form, a large number of image frames are first "folded" into the correlation memory substrate of MHAC, called the **holograph** using a generalized multidimensional differential Hebbian learning algorithm. During the encoding, each image is associated with an index pattern. The associations are stored in the holograph.

The encoder can accept a fuzzy **assertion field**, along with the image, to specify cognitively important regions. The MCN learning algorithm in addition to "enfolding" the individual measurements (in the phase plane) also learns the cognitive importance of the pixel elements (in the magnitude plane).

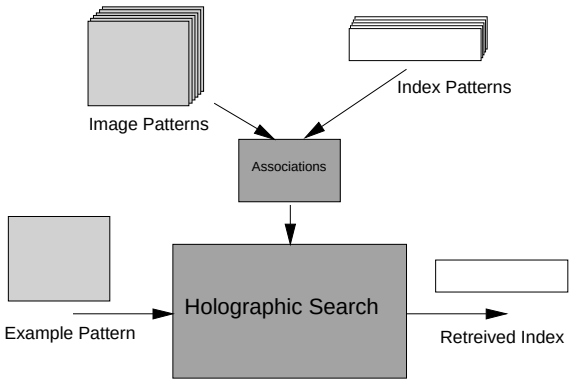

Fig-3 Holographic Query System Outline

During the visual query, similarly, the inquirer provides a sample image and a fuzzy **attention field**. The inquirer can dynamically alter (or compound) the field to focus on any other object.

Once the query pattern is given, the associative search mechanism of MHAC performs an associative recall into the holograph. It returns an index pattern that corresponds to the best match among the previously stored image. As explained before, it evaluates the best match with respect to the objects specified by the attention field.

Corresponding to each decoding operation during pattern search, the recalled output (i.e. the index pattern) similarly contains phases and magnitudes. A vector constructed out of the phase elements now helps us to precisely identify the actual matching image. On the other hand, the magnitude vector corresponds to the MHAC's **confidence field** on the index pattern space. High magnitude of the retrieved index pattern corresponds to potential match. Similarly, low magnitude corresponds to potential absence of the given object in the holographic database.

The obvious advantages of not directly retrieving the images but to go through the indirection of index patterns are twofold. First, although the recalled index patterns may contain some noise but the images are always retrieved crisp. Index patterns can be specially designed and spaced in phase space for symmetry to facilitate noise reduction and removal. The second advantage is holograph size. AS evident from (3) the size of the holograph is the product of the sizes of the two associated patterns. The number of elements in the index pattern can be of logarithmic order with respect to the number of images, which is generally much smaller than the image. For example, if we want to store 1024 images in a holograph, then only 10 element index patterns will be needed assuming most liberal binary spacing. Thus, using index patterns, instead of actual images makes holograph size significantly smaller.

5 TEST RESULTS

The key features and performance of the holographic image archive are now demonstrated through a prototype image archive (MEDIA) which "enfolds" a set of 64 CT-scan/MRI images. Fig-9 shows a few samples from it.

Assertion Based Encoding: Before enfolding, using a Clipped-Gaussian segmentation algorithm the CT-scan/MRI images have been segmented into five segments (i) bone tissue, (ii) soft tissue, (iii) fat tissue, (iv) water and (v) air segments based on their x-ray/electromagnetic refractivity. The membership value of a pixel in a class is defined by four parameters using (8):

$$m_k = m(I_{\min}, I_{\max}, \mu, \sigma) = 1 \qquad \text{when} \qquad I_{\min} \le I_k \le I_{\max}$$

$$= e^{-\frac{(\mu - I_k)^2}{\sigma}} \qquad \text{otherwise.} \qquad \ldots.(8)$$

Fig-10 shows the result for a typical segmented image. Table-1 gives the parameter of segmentation and the cover of the corresponding regions. In this table μ and σ respectively provide the mean and standard deviation of the gaussian segmentation window, and $I_{\max} - I_{\min}$ shows the clipping values. The assertion strength (or cover) is computed as (9):

$$f = \frac{\sum_{n=1}^{N} \lambda_n}{N} \quad \ldots.(9)$$

The first two or three of these segments actually bear cognitive importance to a radiologist. As evident in this example, quite often the large (and statistically dominated) air surrounding the objects of focus, not only is cognitively unimportant, but quite often they create skew in the symmetry of distribution during plain associative encoding. The skew (or asymmetry) of the retrieved patterns are measured using (10).

$$k = \frac{\sum_{m=1}^{N} \gamma_m^e e^{\left(\sum_{j}^{d-1} \hat{i}_j \phi_{j,m}^e\right)}}{N} \quad \ldots.(10)$$

To avoid such unnecessary interference, in MHAC scheme we have enfolded the air image regions with very low assertion. The assertion values of individual pixels are computed from class assertion strength *AF* by (11):

$$\lambda_k^e = AF_{class} \cdot m_k \quad \ldots.(11)$$

Table-1 Segmentation for Plate#50

Region	$I_{\max} - I_{\min}$	μ	σ	*f*
BONE	255-201	255	0.010	0.044
TISSUE	180-150	144	0.015	0.288
FAT	140-080	100	0.010	0.156
LIQUID	045-030	035	0.010	0.167
AIR	025-000	025	0.050	0.320

For comparison, the pixels of air segment have been assigned several assertion values (1,0.5, and 0.1). The reduction of assertion values improved the symmetry of distribution for most of the images. Fig-4 graphically demonstrates how the asymmetry changes for each of these 64 images with the lowering of assertion. For example, for plate #50, the AF=1.0 encoding shows an asymmetry =.28, while with reduced emphasis on air segment, asymmetry becomes as low as .02. Few of the plates which do not have large air segment (such as plates #1, #2, #3, etc) show smaller change in asymmetry value.

The benefit of variable assertion enfolding on holographic memory performance is demonstrated in Fig-5 which plots the average accuracy for all of these patterns. As evident, such shielding not only reduces the saturation of the memory but also improves the quality of recalled information by reducing the amount of interference from image segments, which can be stripped at the encoding stage.

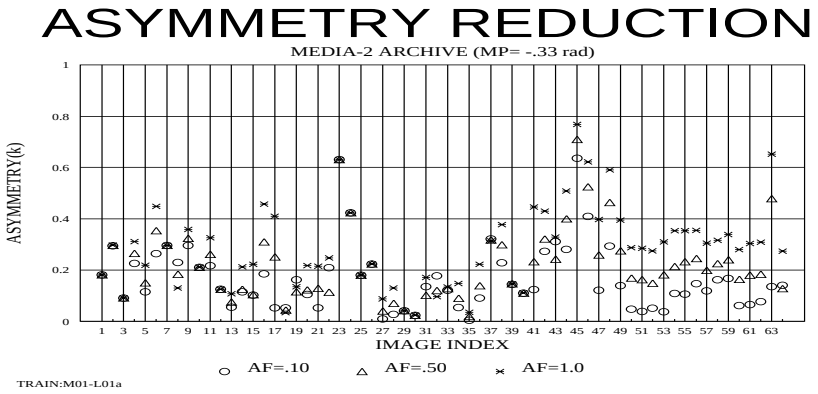

Fig-4 Asymmetry Reduction by Reducing the Assertion on Air Segment

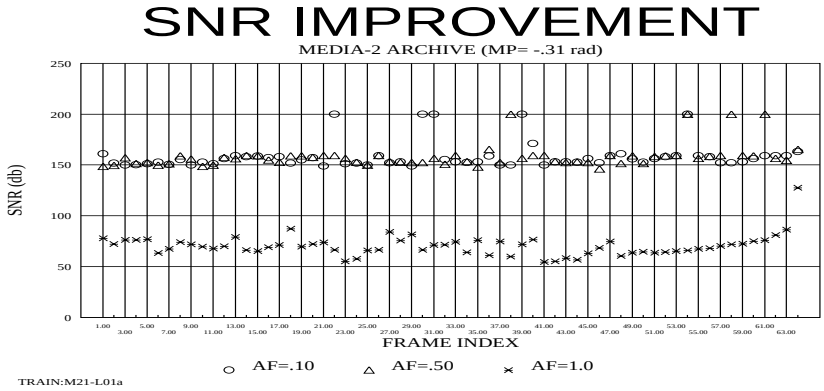

Fig-5 Recall Performance

Attention Based Query: Two sets of tests have been performed to characterize the behavior of MHAC when attention spans and locations are varied. Fig-6 respectively show the scheme of attention windowing for these tests. Fig-7 shows the result when during the retrieval the attention on the query pattern has been varied from 60x60 pixels to 110x110 pixels in 6 steps. It is called ZOOM test. Fig-8 shows the result when instead of using attention windows of different sizes, they were selected from different locations of the query image frame (with fixed size 55x55 pixels). Both of the figures plot the average retrieval accuracy in the bar-plot (left y-scale) and the corresponding size of the focus window (mean focus MF) in the line-plot (right y-scale). The three bar sets denote the accuracy for three assertion values for the air segment used during training.

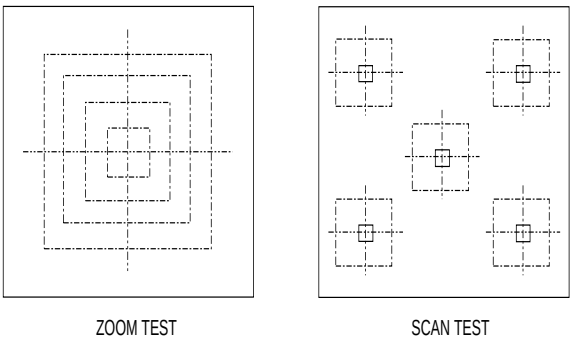

Fig-6 Scan and Zoom Tests

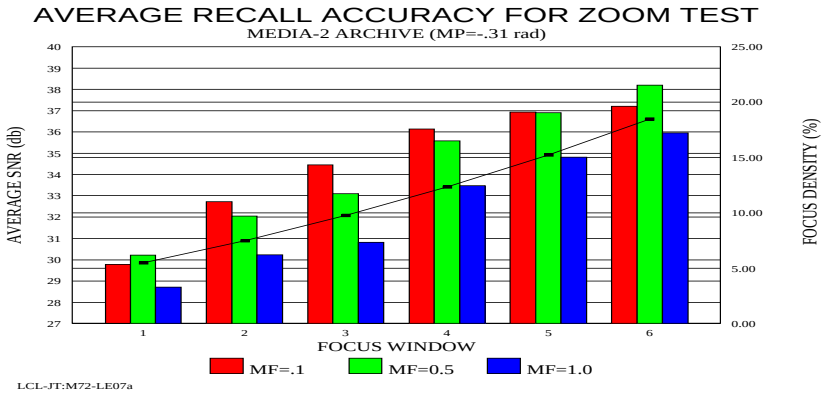

Fig-7 Recall Performance for Sizes of Focus Window

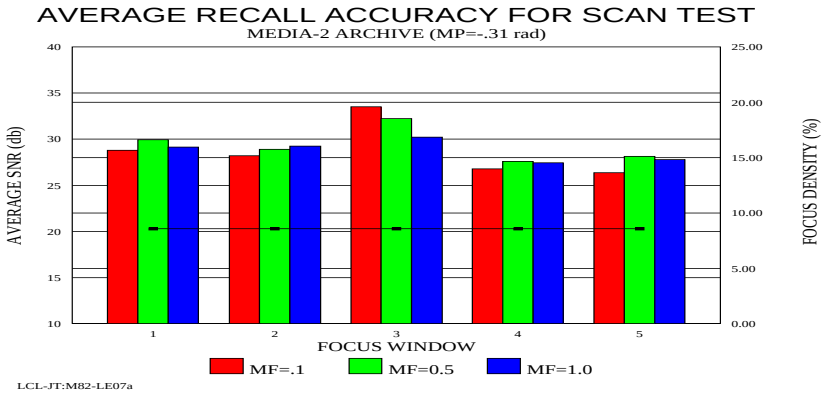

Fig-8 Recall Performance for Locations of Focus Window

As evident, the retrieval accuracy remained well above 20-25db even for attention window lower than 10% of the total frame. This is remarkably different from conventional AAMs, which show sharp cutoff when the number of dissimilar bits reaches 50% irrespective of their sophistication. Also evident in these graphs is that despite the loss of information during low assertion encoding relatively little performance was lost. This is due to the fact that the information that has been dropped (air segment) by low assertive encoding was inherently unusable. In Fig-8 it is also evident that the accuracy of retrieval is in general high in the center (number 3) window. This conforms to the general nature of CT and MRI images where the objects of cognitive importance are always centered.

Fig-11 illustrates an example of query. Fig-11(a) is a sample query pattern with an attention windows emphasizing *Jugular-Foramen and Carotid Canal* region. Although the window looks rectangular, but in actuality a clipped Gaussian range filter analogous to (8) has been used to gracefully smooth away the boundaries. Table-2 shows the clipping boundaries of this window and corresponding smoothing function of the attention strength.

The images retrieved by the search method corresponding to these attention shields are shown in Fig-11(b) and (c). Two correct matches for this query are plat #34, and at plate #33. As explained earlier in section 4, these matching images have been retrieved through recalling their index patterns.

A conventional AAM cannot be used for such search. Because, in the first place, without the ability of match space localization, it will never converge to different matching pattern images beginning from the one sample pattern image.

MNC feedback based interactive Search: The MNC feedback is the behind the scene capability which actually makes the construction of a functional search engine out of MHAC possible. It's role is explained now.

If we consider a conventional AAM, which just produces a mono-modal output pattern (for example any AAM based on ANN), during recovery we will never be sure if that retrieval is correct or not. Thus, they can not be used for any effective search.

In contrary, during every retrieval MHAC generate an index pattern in the output, elements of which have both phase and magnitude. Overall low magnitude of the pattern corresponds to the absence of a match. We use a measure analogous to (9) called *Mean Normalized Confidence* (MNC) to quantify it. An event of no match or wrong retrievals is always directly correlated by a corresponding low MNC (or high doubt). MHAC thus provides meta-information about the validity of each of the retrieved pattern.

Due to it's complex representation, a match in holographic model is analogous to a wave *resonance* between a query and a previously stored pattern. This resonance capability is one of the fundamental (as well as distinguishing) feature of MHAC which makes it possible to use it as a functional search engine.

The critical need of this capability is further illustrated by explaining the process of translated search. As can be seen in Fig-11, the object of interest in the query pattern is spatially translated compared to the matching sub-pattern in the target. Any translated search requiring multiple decoding needs a feedback to evaluate the presence of match in candidate locations. For associative search, this feedback is needed in addition to the regenerated retrieved pattern.

We have used a 10x10 pixel grid space to converge to the correct spatial location in the holograph. The match was sensed by a process of resonance through MNC feedback. Fig-12 plots the MNC feedback obtained from the memory by resonating the query sample at various spatially translated grid locations of the holograph. Sharp resonances are detected from the holograph at displacements (-10,100) and (130,-20). These indicate the presence of matching patterns in these locations in the images enfolded beneath.

As evident visually in Fig-12 as two sharp peaks, these correspond to the two correct matches (plates #34, and #33 of Fig-11). On the one hand, the MNC feedback at the meta-plane provides the resonance strength indicating the spotting of a match, on the other hand, the phase plane provides the associated index pattern, revealing the identity of the matching image. Conversely, the characteristically low resonance at other grid locations tells the external searcher about the absence of matches in those locations.

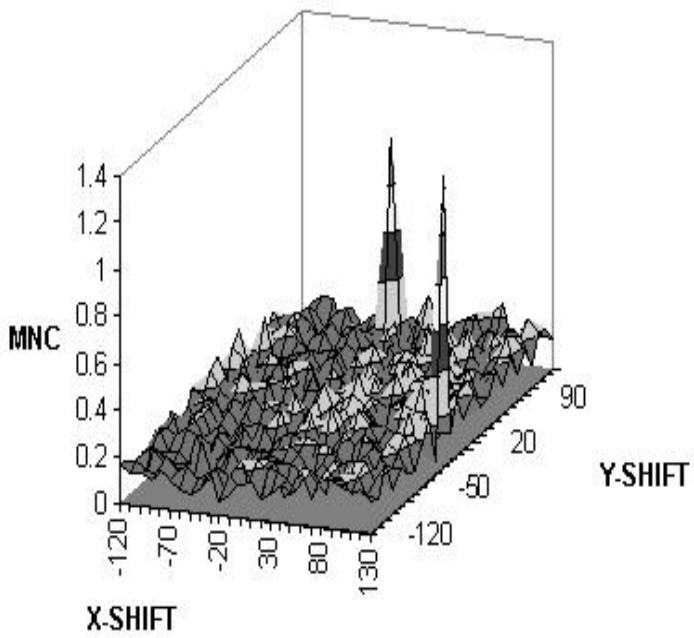

Fig-12 Mean Normalized Confidence (MNC) Response at Grid Points

Table-2 Masks for Object of Focus in the Query

X range	74-021
Y range	146-093
focus cover	.044

Table-3 Query Results for Jugular Foramen and Carotid Canal Query

Match#	Image	Shift(x,y)	SNR (db)	MNC
1	A34	130,-20	31.92	1.095
2	A33	-10,100	37.46	1.183

This example of translated pattern search also reveals another important advantage of holographic method. In a conventional search, a translated pattern match needs searching in all locations of all the images. In contrast, in holographic method that process is dramatically reduced into the process of searching only on a single holographic plane. Table-3 shows the search performance for our query shown in Fig-11. Similar to this example, it has been observed that response patterns can be retrieved with more than 30db signal to noise ratio for attention field covers as low as 5-15%.

Feedback like MNC resonance is a natural as well as essential part of any search mechanism that would deal with imperfect information. Current AAMs do not have this critical capability within its mono-modal framework of information representation, and thus can not be used for multistage interactive search.

6 CONCLUSIONS

In this paper we have presented the conceptual and analytical model of the holographic associative memory. It can process meta-component of information in the forms of assertion, attention and confidence. It has been analytically demonstrated how each of these notions can be supported within a representational framework of holographic computation. Also it has been demonstrated with example how each of these meta-quantities and corresponding processing ability can be used to construct an intermediate annotationless content-based search strategy. From the point of view of associative computing, this new memory advances the state by presenting a new associative memory form with has the ability to process these meta-quantities. From the point of view of the image database, this provides the first CBIR technique which is based on associative computing. The advantage of this method is that it enables dynamic handling of the object concepts. In contrast, in the traditional intermediate model based CBIR approaches objects are needed to be predefined at the time of encoding. The proposed technique otherwise retains the usual advantages of parallel and distributed associative computing.

Parallelizability: For the ease of illustration of various aspects of this novel CBIR technique we have presented a case with 64 images. But extensive simulations have confirmed the scalability of this approach to larger cases. As an example, it has been demonstrated that 1000-2000 images with 4K pixels each can be associatively enfolded on a single MHAC memory of 12K bytes and can be recalled with less than 4% error [12]. As evident in equations (3) and (4), the search time in MHAC is always independent of the number of stored images and always takes *mxnxn* complex operations per pattern decoding. It is comparable to template matching cost with three images for 2D representation [12]. Such single step retrieval can be very important for many image recognition applications which are based on real-time template matching. Also evident in (3) and (4) that the involved computations are highly parallelizable with straightforward mapping. The training process is also similarly highly parallelizable. It takes *mxn* complex operations pattern encoding. Generally, training by differential encoding converges within 10 cycles [12].

Object-Orientedness in Distributed Associative Computing: It would be appropriate in this concluding discussion to illustrate the meaning of "object-ness" as provided by this associative memory. Traditionally, objects refer to a rational and well contained partition in a structured information space. For the symbolic world, the structure as well as the containment rationale of this subspace are precisely defined (with records, fields, slots, attributes, etc). However, such definiteness, either in rationale or in structure, can not be assumed for image information.

For example, in the query image shown in Fig-11(a)], there is little possibility that two interpreters will use the same defining window or even same vocabulary when defining the object *Jugular-Foramen and Carotid Canal* (such as one can use "the region around *Jugular-Foramen*"). The relationships among these objects are also similarly subjective. Despite such subjectivities in the definitions of these index concepts, an intermediate model based approach has to guess these interpretations (and make choices) from the very beginning during model building, which is quite unrealistic.

For being "object-oriented" in such an amorphous target information space, what is required is a formalism with which subspaces (such as the region around Carotid Canal) can be defined dynamically with allowance for approximation and still the amorphous pattern space can be accessed and searched with reasonable computational efficiency. Holographic associative computing tries to provide exactly this form of localized access capability. Traditional AAMs

provide the allowance for approximation but cannot provide the localization which is central to the concept of "object-ness". The capability of search localization provided by this memory brings the current state of distributed and parallel models of associative computing one step closer to the applications requiring object-oriented access.

Meaning and Content: One of the fundamental difference between this approach and the conventional CBIR approaches is in the way that they attach "meaning" to the content[7]. In the conventional approaches, all meaning have to be attached in advance during encoding (or archiving) either by human or by automatic extraction of a set of predefined features. MHAC, by way of assertion, allows attachment of predefined meaning for that part of the contents about which the encoder is confident. However, it does not force archive to interpret everything. For the more difficult subjective part of the content, by way of attention MHAC allows attachment of meaning dynamically during query.

Interestingly, MHAC can be used as an assisting tool for the intermediate model based approaches in the encoding or annotation stage. These model-based approaches too require the features to be extracted in advance during the encoding. Such automatic index extraction requires expensive template search in the images. MHAC search engine can speedup such template matching.

The issue of content based search in images is closely related to understanding our own mechanism of representation and perception. Most likely there is no single best solution. Conventional model based approaches tend to be more useful for applications where the image concepts are well defined and extensive domain-specific modeling is possible. Images of graphical nature, such as texts, maps, circuit drawing, etc. tend to fall in such category. In contrast, the approach demonstrated in this work has its advantage when the objects are difficult to describe or model, the content does not show any unambiguously distinguishable structure, the volume of images is enormous, and examples with visual similarity at the object level are available. Medical diagnostics imagery, stellar images, fingerprint, satellite or planetary landscape images tend to fall in this category.

6.1 Acknowledgement

This research has been supported by a doctoral fellowship by the East West Center of Hawaii. Also a part of this research has been funded by DARPA research grant no DABT 63-93-C-0056.

7 REFERENCES

1. Cahill, D. R. & Orland M. J., *Atlas of Human Cross-Sectional Anatomy*, Lea & Febiger, Philadelphia, 1984.
2. Chang, S.K., Arding Hsu, "Image Information Systems: Where Do We Go From Here?", *IEEE Trans. on Knowledge and Data Engineering*, v.4, n.5, October 1992, pp431.
3. Chang, S. K., C. W. Yan, D. Dimitroff, T. Arndt, "An Intelligent Image Database System", *IEEE Trans. on Software Engineering*, v.14, n.5, pp681, May 1988.
4. Gabor, D., "Associative Holographic Memories", *IBM Journal of Research and Development*, 1969, I3, p156-159.
5. Gupta, A., T. Weymouth, R. Jain. semantic Queries in Image Databases, E. Knuth, L. M. Wegner (eds.), *IFIP Trans. on Visual Database Systems*, II, A7, 1992, pp201-215
6. Halin, G., N. Mouaddib, "An Object Oriented Approach to Design a Content-Based Image Retrieval Model", *Image Storage and Retrieval Systems*, SPIE, v.1662, pp100, 1992.

---

7 On this matter, one of the pioneers in this field, S. K. Chang in an evaluation report titled "Where Do We Go From Here?" wrote [2]: "Spatial entities (object) and relationships (image features) in image do not carry any semantic meaning by themselves.. Associating semantic meanings by naming will cause some problems with image information. First, the same image could be interpreted in different ways. Second, the same image could be used in different ways during different time periods. ... directly associating semantic meanings to image entities and relationships will severely limit the usage of image information".

7. Hibler, J. D., C. H. C. Leung, K. L. Mannock, M. K. Mwara, "A System for Content-Based Storage and Retrieval in an Image Database", *SPIE, V1662 Image Storage and Retrieval Systems*, pp80, 1992.

8. Hinton, G.E., J. A. Anderson, *Parallel Models of Associative Memory*, Lawrance Erlbaum, NJ, 1985.

9. Hu, M. K., "Visual Pattern Recognition by Moment Invariants", *IRE Transactions on Information Theory*, IT-8, 1962, pp28-32.

10. Iyenger, S.S., R. L. Kashyap, "Guest Editors' Introduction on Image databases", *IEEE Trans. on Software Eng.*, v.14, n.5, pp608-609, May 1988.

11. Joseph, T., A. F. Cardenas, "PICQUERY: A High Level Query Language for Pictorial Database Management", *IEEE Transactions on Software Engineering*, v.14, n.5, pp630, May 1988.

12. Khan, J. I., "Attention Modulated Associative Computing and Content Associative Search in Images", *Ph.D. Dissertation*, Department of Electrical Enginnering, University of Hawaii, July, 1995.

13. Khan J. I.,& D. Yun, "Searching into Amorphous Information Archive", *International Conference on Neural Information Processing*, ICONIP'94, Seoul, October, 1994, pp739-749.

14. Kumar, B. V. K. V & P. K. Wong, "Optical Associative Memories", *Artificial Neural Networks and Statistical Pattern Recognition*, I. K. Sethi and A. K. Jain (Editors), Elsevier Science Publishers, pp219-241, 1991.

15. Masters, T., *Signal and Image Processing with Neural Networks*, John Wiley & Sons, New York, 1994.

16. Flickner, M,, H. Sawheney, W. Niblack, et al., "Query by Image and Video Content: The QBIC System", *IEEE Computer*, Sept. 1995, v.29, n.9, pp23-31, 1995.

17. Rabitti, F., P. Savino, "Automatic Image Idexation to Support Content-Based Retrieval", *Information Processing & Management* v.28 n.5, pp547, 1992.

18. Sutherland, J., "Holographic Models of Memory, learning and Expression", *International J. Of Neural Systems*, 1(3), pp356-267, 1990.

19. Tai, Heng-Ming, T. L., Jong, "Information Storage in High-order Neural Networks with Unequal Neural Activity", *J. Of Franklin Institute*, v.327, n.1, 1990, pp16-32.

20. Tucci, M., G. Costagliola, S. K. Chang, "A Remark on NP-Completeness of Picture Matching", *Information Processing Letters*, v.39, n.5, pp241, September 1991.

21. Turtur, A., F. Prampolini, M. Fantini, R. Guarda, M. A. Imperato, "IDB: An image database system", *IBM Journal of Research & Development*, v.35, n,1/2, pp88, January/March 1991.

22. Yamane, J., M. Sakauchi, "A Construction of a New Image Database System which Realizes Fully Automated Image Keyword Extraction", *IEICE Trans. Infor. & Sys.*, v.E76-D, n.10, pp1216, October 1993.

23. Chang, N.S., K.S.Fu, "Picture Query Languages for Pictorial Data-Base Systems", *Computer*, November 1981, pp23.

24. Crehange, M., Malika Smail, "INTERACTIVITY and HYPERTEXT APPROACH in IMAGE RETRIEVAL: the EXPRIM process, the RIVAGE system", *SPIE v. 1662, Image Storage and retrieval Systems*, 1992, pp124-133.

25. Hasegawa, J., N. Okada, J. Toriwaka, "Intelligent Retrieval of Chest X-Ray Image Database Using Sketches", *Systems and Computers in Japan*, v.20, n.7, pp29, 1989.

26. Kato, T., "Database Architecture for Content-Based Image Retrieval", *SPIE, V1662 Image Storage and Retrieval Systems*, pp112, 1992.

27. Narashimhalu, A. D. Guest Editors, "Special Issue on Advances in Visual Information Management Systems", ACM Multimedia Systems, v.3, n.1, Feb 1995.

28. Gudivada V. N., & V. J. Raghavan, "Content-Based Image Retrieval Systems", IEEE Computers, Sept. 1995, v.29, n.9, pp18-22.

29. Ogle, V., & M. Stonebraker, "Chabot: Retreival from a Relational Database of Images", *IEEE Computers*, Sept. 1995, v.29, n.9, pp40-48.

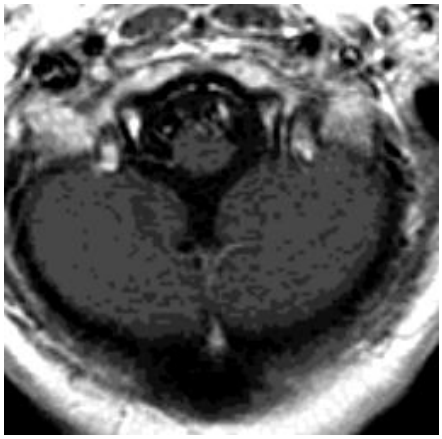

SKL−DN:A33:256x256

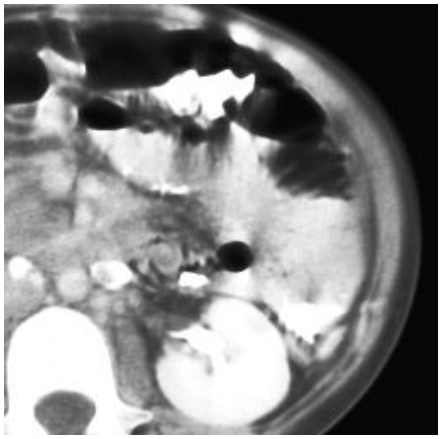

ABD−RT:A26: 256x256

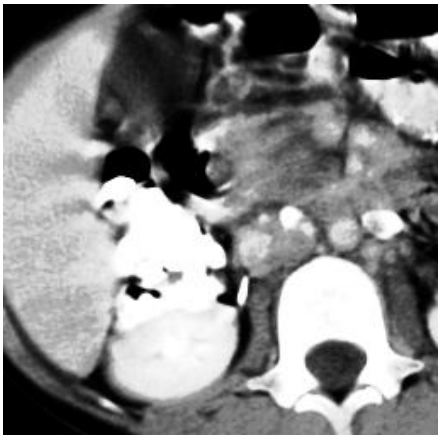

ABD−LT:A25:256x256

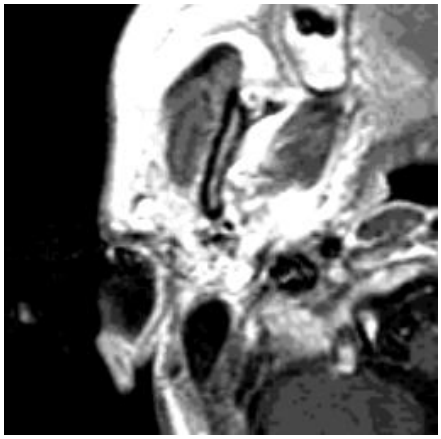

SKL−UL:A34:256x256

Fig−9 Some Samples of Images Stored in the Archive

(a) CT scanned image

(b) Bone segment

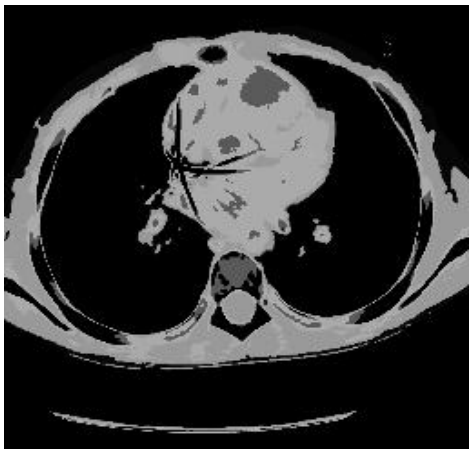

(c) Soft tissue segment

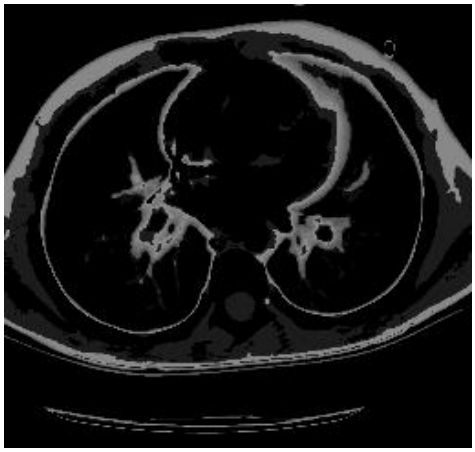

(d) Fat tissue segment

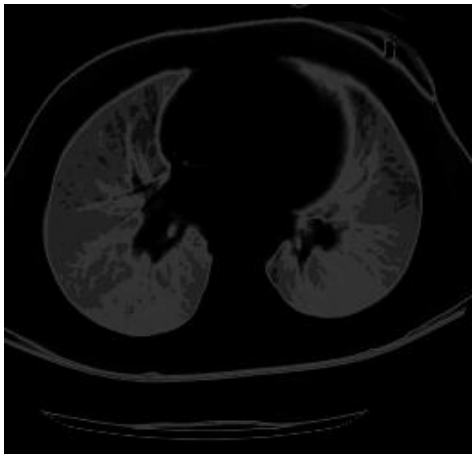

(e) Liquid segment

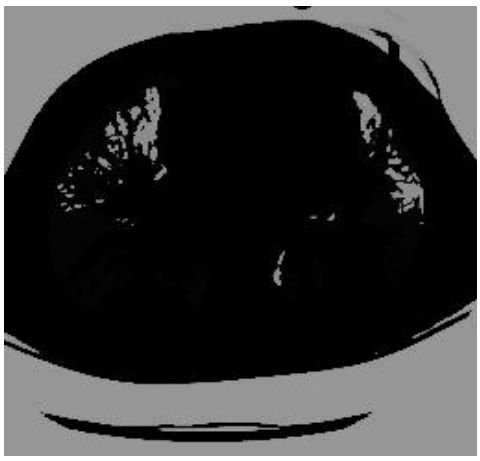

(f) Air segment(negative)

Fig−10 Segmentation based on Tissue Types

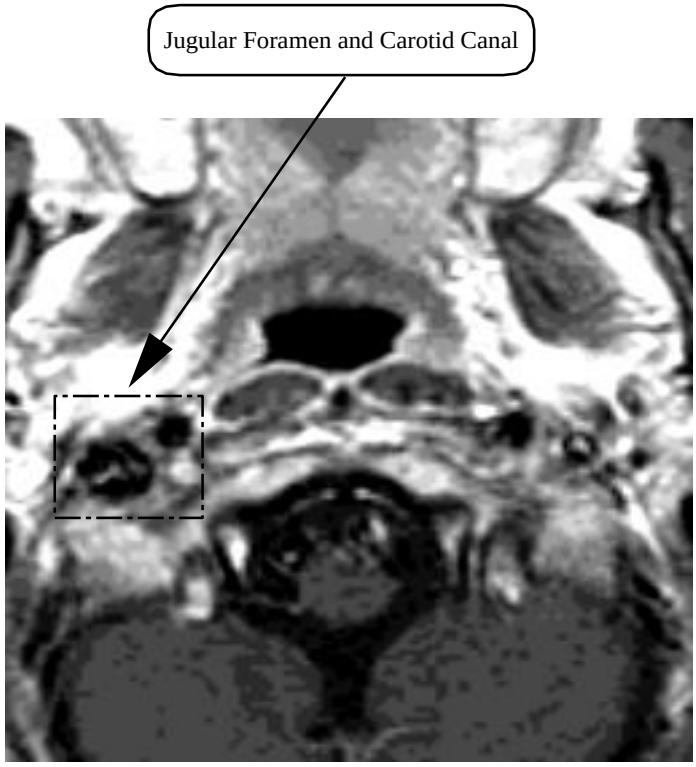

SKL−Q1 256x256 MRI

Fig− 11(a) Query Pattern with Focus

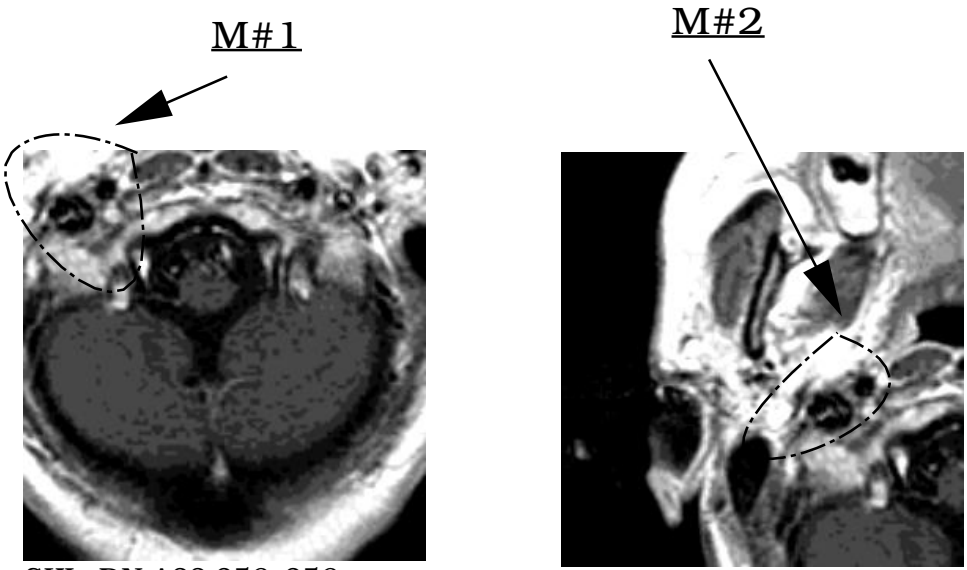

SKL−DN:A33:256x256

SKL−UL: A34: 256x256

Fig−11(b) Image Patterns corresponding to retrieved Index Patterns